Highly Efficient Light-Emitting Diodes with Microcavities

E. F. Schubert,* N. E. J. Hunt, M. Micovic,† R. J. Malik, D. L. Sivco, A. Y. Cho, G. J. Zydzik

One-dimensional microcavities are optical resonators with coplanar reflectors separated by a distance on the order of the optical wavelength. Such structures quantize the energy of photons propagating along the optical axis of the cavity and thereby strongly modify the spontaneous emission properties of a photon-emitting medium inside a microcavity. This report concerns semiconductor light-emitting diodes with the photon-emitting active region of the light-emitting diodes placed inside a microcavity. These devices are shown to have strongly modified emission properties including experimental emission efficiencies that are higher by more than a factor of 5 and theoretical emission efficiencies that are higher by more than a factor of 10 than the emission efficiencies in conventional light-emitting diodes.

Fabry-Perot cavities are optical resonators defined by two coplanar reflectors separated by a macroscopic distance (*1*). If this distance is small, namely one half or one single wavelength of operation (that is, on the order of 1 μm for visible and near-infrared light), the cavities are called optical microcavities. The density of optical modes within a microcavity is strongly modified as compared to the mode density in free space surrounding the cavity: The cavity allows for the propagation of optical waves only at the fundamental resonance mode and its harmonics along the optical axis of the Fabry-Perot microcavity. Modes other than the fundamental resonance and its harmonics are not supported by the cavity, and such modes are disallowed. The energy of photons confined to the microcavity is thus quantized, in near perfect analogy to the quantization of electron energy inside a quantum well potential.

Intriguing physics evolves if an optically active medium, that is, a photon-emitting medium, is placed between the two reflectors of a coplanar Fabry-Perot microcavity.This novel field of condensed matter research has, during the past few years, made possible a new generation of microresonator devices and the exploration of new quantum electrodynamic phenomena (*2*, *3*). Several microcavity geometries have been used, including planar (Fabry-Perot) microcavities, spherical resonators, disk-shaped resonators, and fully three-dimensional resonators (*2*–*6*). The optically active materials inside the microcavity structures included optically active rare-earth atoms, semiconductors, and dyes (*7*–*11*).

In this report we demonstrate that microcavity physics can be exploited in devices whose properties are superior to those of conventional devices. We show that a type of light-emitting diodes (LEDs) that use microcavity effects has clearly improved characteristics as compared to conventional LEDs.

Of particular interest for the technological application of microcavity effects is the enhancement and suppression of radiation. This interest is based on the fact that the optical emission rate in microcavities along the cavity axis can be enhanced under certain experimental conditions, which will be defined below. To illustrate this effect, we consider the semiconductor microcavity shown in Fig. 1, which consists of two reflectors, namely, an Ag mirror and a distributed Bragg reflector (DBR). The reflectivity of the semiconductor-silver interface is 96% for near-infrared light. The 90% reflective DBR consists of 10 pairs of an AlAs/GaAs multilayer structure with each layer being λ/4 thick, where λ is the resonance wavelength of the cavity. Because the DBR reflectivity is lower than the reflectivity of the Ag mirror, photons will escape from the cavity mainly through the DBR. The active region of the cavity contains four $In_{0.15}Ga_{0.85}As$ quantum wells.

The enhancement of the emission intensity along the optical axis of the cavity can be calculated in terms of Fermi's Golden Rule (*12*). At the resonance wavelength, the emission enhancement factor is given by (*13*)

$$G_e = \frac{\xi}{2}\frac{(1+\sqrt{R_2})^2(1-R_1)}{(1-\sqrt{R_1R_2})^2}\frac{\tau_{cav}}{\tau} \quad (5)$$

where R_1 and R_2 are the reflectivities of the mirrors and, because we assume $R_1 < R_2$, most light exits the cavity through the reflector with reflectivity R_1. The antinode enhancement factor ξ has a value of 2, if the active region is located exactly at an antinode of the standing optical wave inside the cavity. The value of ξ is unity, if the active region is smeared out over many periods of the optical wave, and ξ is 0 if the active region is located exactly at an optical node. Calculations of the radiative lifetime τ_{cav} for the structure revealed that it is changed by less than 10% relative to the spontaneous lifetime τ, that is, $\tau_{cav} \cong \tau$ (*13*, *14*). Equation 1 allows us to calculate the on-resonance enhancement, and using $\xi = 1.7$ one obtains $G_e = 67$ for the structure shown in Fig. 1.

The total enhancement integrated over all wavelengths, rather than the enhancement at the resonance wavelength, is relevant for practical devices. Exactly on resonance, the emission is enhanced along the axis of the cavity. However, off resonance, the emission is strongly suppressed. Because the natural emission spectrum of the active medium (without cavity) may be much broader than the cavity resonance, it is, a priori, not clear if the integrated emission is enhanced at all. To calculate the integrated enhancement, the spectral width of the cavity resonance and the spectral width of the natural emission spectrum must be determined. The former can be calculated from the uncertainty relation and the pho-

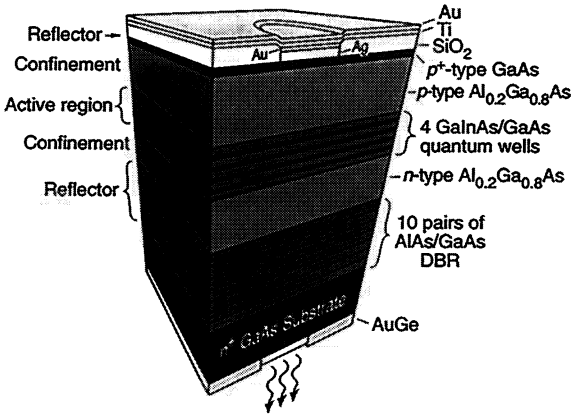

Fig. 1. Layer sequence and structure of the resonant-cavity LED. The planar semiconductor microcavity is defined by a DBR and an Ag mirror. The circular Ag reflector also serves as ohmic contact. Light emission occurs through the substrate coated with an antireflection film.

AT&T Bell Laboratories, Murray Hill, NJ 07974, USA.

*To whom correspondence should be addressed.
†Present address: Department of Electrical Engineering, Pennsylvania State University, University Park, PA 16802, USA.

ton lifetime in the cavity, τ_{ph}, according to $\Delta E = \hbar/\tau_{ph}$ or

$$\frac{\Delta\lambda}{\lambda} = \frac{\lambda}{2nL_{cav}}\left[\frac{1-\sqrt{R_1R_2}}{\pi(R_1R_2)^{1/4}}\right] \quad (6)$$

where L_{cav} is the effective cavity length and n is the refractive index in the cavity. For typical reflectivities of $R_1 = 90\%$ and $R_2 = 96\%$ and an L_{cav} value of $2.7(\lambda/n)$, the spectral width is $\Delta\lambda \cong 5$ nm at $\lambda = 900$ nm (*13*). The theoretical width of the emission spectrum of bulk semiconductors is $1.8\ kT$ (*15*), where k is the Boltzmann constant and $T = 300$ K. The value of $1.8\ kT$ corresponds to a width of the natural emission spectrum from a bulk semiconductor, $\Delta\lambda_n$, of 31 nm at an emission wavelength of 900 nm (where n is the refractive index). Thus, only a small part of the spectrum is strongly enhanced, whereas the rest of the spectrum is suppressed. The integrated enhancement/suppression ratio can be calculated by assuming a Gaussian natural emission spectrum (*13*)

$$G_{int} = G_e\sqrt{\pi \ln 2}(\Delta\lambda/\Delta\lambda_n) \quad (7)$$

For the above values of G_e, $\Delta\lambda$, and $\Delta\lambda_n$, we deduce an integrated enhancement of $G_{int} \cong 16$. The value of G_{int} can be quite different for different types of materials. Narrow atomic emission spectra can be enhanced by several orders of magnitude (*7*). On the other hand, materials having broad emission spectra such as dyes or polymers (*10*) may not exhibit any integrated enhancement at all.

A significant difference exists between LEDs used for display purposes and those used for optical fiber communication. The figure of merit for communication LEDs is the photon flux density per unit solid angle. A high photon flux density allows one to couple much of the emitted light into an optical fiber. For display LEDs, the figure of merit is the total power emitted into the hemisphere of the observer; that is, the total number of photons rather than the photon density is relevant. Several structures were proposed and realized to improve the efficiency of LEDs, including spherical shapes (*16*), multiple surfaces (*17*), reflectors (*18*), and nonplanar surfaces (*19*). However, none of these concepts can fundamentally modify the photon flux density emanating from the active region but are rather standard geometric optical constructions.

An LED structure that provides an enhanced photon flux density is the resonant-cavity light-emitting diode (RCLED) shown in Fig. 1. The RCLED is a *pn* junction diode integrated with a microcavity. The fundamental mode of the cavity is in resonance with the light-emitting active region of the diode. The active region emits at 930 nm where all other materials used in the structure are transparent. Most light escapes from the cavity through the bottom reflector, because its reflectivity is less than that of the top Ag reflector. The top Ag reflector also serves as a nonalloyed ohmic contact to the heavily doped top p^+-type GaAs layer. The thicknesses of the two confinement layers are chosen in such a way as to (i) have the fundamental mode of the cavity at 930 nm and (ii) place the active GaInAs region into an optical antinode of the cavity. Light exits the structure through the substrate. The exit window is covered with an antireflection coating. A coating of AuGe surrounding the optical window provides an ohmic contact to the n^+-type GaAs substrate.

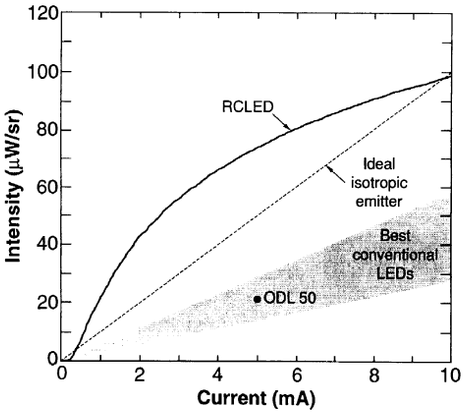

Fig. 2. Light intensity versus current for a planar RCLED emitting at 910 nm; contact diameter, 21 μm; $T = 20$°C. Also shown is the theoretical curve of the ideal isotropic emitter, which is an upper limit for all conventional LEDs. The shaded area indicates experimental intensities of the best conventional LEDs and of the ODL 50, which is a commercial product.

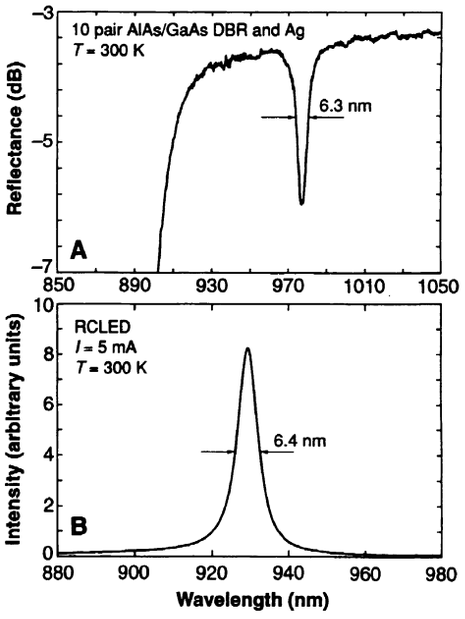

Fig. 3. (**A**) Reflection spectrum from a semiconductor microcavity and (**B**) emission spectrum from a microcavity structure. The similarity of the two spectra shows that optical emission is restricted to the fundamental cavity mode.

The figure of merit of LEDs used in optical fiber communication systems is the photon flux density emitted from the diode at a given current, which, for a given wavelength, will be discussed in terms of microwatts per steradian. The optical power coupled into a fiber is directly proportional to the photon flux density.

The intensity of the RCLED as a function of the injection current is shown in Fig. 2. For comparison, we also show the calculated intensity of an ideal isotropic emitter, which is a hypothetical device. It is assumed to have an internal quantum efficiency of 100% and to be clad by an antireflection coating providing $R = 0$ for all wavelengths emitted from the active region. If the photon emission inside the semiconductor is isotropic, then the optical power per unit current per unit solid angle normal to the planar semiconductor surface is given by

$$\frac{P_{optical}}{\Omega} = \frac{1}{4\pi n^2}\frac{2\pi\hbar c}{e\lambda} \quad (8)$$

where Ω represents the unit solid angle, n is the refractive index of the semiconductor, c is the velocity of light, e is the electronic charge, and λ is the emission wavelength in air. Equation 4 is represented by the dashed line in Fig. 2. Neither the 100% internal quantum efficiency nor such a hypothetical antireflection coating can be reduced to practical levels for fundamental reasons. Therefore, the ideal isotropic emitter represents an upper limit for the intensity attainable with any conventional LED. In fact, the best conventional LEDs have intensities lower than that of the ideal isotropic emitter. Also included in Fig. 2 is the state-of-the-art ODL 50 GaAs LED used for optical fiber communication (*20*). All devices shown in Fig. 2 have planar light-emitting surfaces, and no lensing is used.

Figure 2 reveals that the RCLED provides unprecedented intensities in terms of both absolute values and slope efficiencies. The slope efficiency is 7.3 times the efficiency of the best conventional LEDs and 3.1 times the calculated efficiency of the ideal isotropic emitter. At a current of 5 mA, the intensity of the RCLED is 3.3 times that of the best conventional LEDs including the ODL 50. The unprecedented efficiencies make the RCLED very promising for optical interconnect systems, which will be discussed below.

The RCLED presented here has been designed for an operating current of 5 mA and for use with optical multimode fibers with a core diameter of 62.5 μm. At higher currents, the RCLED intensity starts to saturate as shown in

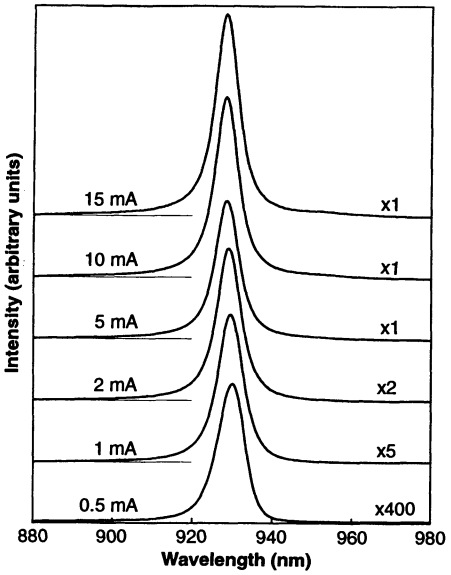

Fig. 4. Emission spectra of an RCLED at different excitation currents (T = 300 K). The spectral shape is independent of the current (given above each trace), indicating the absence of stimulated emission or superluminescence.

Fig. 2. The saturation was shown to be due to band filling (*21*).

At operating voltages of 1.5 V, the electrical power consumed by the devices is 7.5 mW. Less than 7.5 mW is converted to heat. Heating of linear arrays of devices separated by 2 × 62.5 μm = 125 μm is not a problem.

The reflection and emission properties of the RCLED are shown in Fig. 3, A and B. The reflection spectrum of the RCLED (Fig. 3A) exhibits a highly reflective band for wavelengths >900 nm and a dip of the reflectivity at the cavity resonance. The spectral width of the cavity resonance is 6.3 nm. The emission spectrum of an electrically pumped device, shown in Fig. 3B, has nearly the same shape and width as the cavity resonance width.

In conventional LEDs, the spectral characteristics of the devices reflect the thermal distribution of recombining electrons and holes in the conduction and valence bands. The spectral characteristics of light emission from microcavities are as intriguing as they are complex (*22*). However, restricting our considerations to the optical axis of the cavity simplifies the cavity physics considerably. If we assume that the cavity resonance is much narrower than the natural emission spectrum of the semiconductor, then the on-resonance luminescence is enhanced whereas the off-resonance luminescence is suppressed. The on-axis emission spectrum should therefore reflect the enhancement, that is, the resonance spectrum of the cavity. The experimental results shown in Fig. 3 confirm this conjecture.

Microcavities provide enhanced optical feedback through photons oscillating in the cavity. The enhanced photon density results in a higher probability of stimulated emission processes. To test the relevance of stimulated emission processes, we measured the RCLED spectrum at different excitation intensities (Fig. 4). For injection currents ranging from 0.5 to 15 mA, the optical spectra are virtually the same, indicating the insignificance of stimulated emission.

A design criterion for the RCLED is $(1 - R_1) \gg \alpha \ell_{active}$, where α is the absorption coefficient and ℓ_{active} is the thickness of the active region. This condition ensures that the exit-mirror loss is much larger than self-absorption in the active region. If the above criterion were not fulfilled, the RCLED would provide a lower intensity enhancement or no enhancement at all. On the other hand, laser oscillation requires that the round-trip gain exceeds the mirror loss. The maximum gain of a population-inverted structure cannot exceed the magnitude of the absorption in the structure, that is, $|g| \leq |\alpha \ell_{active}|$ (*23*). Thus, the maximum achievable gain is always smaller than the mirror loss, irrespective of the pump level, which shows that laser oscillations cannot occur in RCLEDs.

Optical sources based on spontaneous and stimulated emission, such as LEDs and lasers, form the basis of all silica fiber communication. In practice, LEDs are preferred over lasers whenever possible, for three major reasons. First, LEDs have much higher reliability, which can exceed that of lasers by one order of magnitude (*16*, *24*). Second, the temperature sensitivity, which is known to be governed by the well-known T_0 law in lasers, is smaller for LEDs (*24*). Third, the simpler fabrication process of LEDs results in lower production cost. However, LEDs cannot be used in high bit rate (>1 Gbit) and long-distance (>5 km) communication.

Several intriguing devices have been proposed or realized during the last 5 years. They include the vertical-cavity surface-emitting lasers (VCSEL) (*25*), the zero-threshold laser (*3*, *26*), the microdisk laser (*2*, *27*), photon-recycling LEDs (*19*), and the single-mode LED (*28*). Most of these devices are near-unity β devices (*2*, *3*), where β is the spontaneous emission factor, which gives the fraction of photons coupled into a single optical mode. To achieve this goal, the volume of the device must be reduced to a very small size (*2*). The required current densities in such devices are impractical for any reasonable optical output.

Photon recycling LEDs (*19*) provide very high external quantum efficiencies but are useful for display rather than optical interconnect applications. Photon recycling prolongs the effective recombination lifetime of free carriers, and, as a result, photon recycling LEDs are slow. Although this factor excludes such LEDs for high-speed applications, the slow speed is compatible with display applications.

The VCSEL is considered a potential candidate for optical interconnect systems. At first glance, the basic structures of the VCSEL and the RCLED are similar. However, the VCSEL does not fulfill the RCLED design criterion $(1 - R_1) \gg \alpha \ell_{active}$. As a result, the VCSEL has light output intensities in the spontaneous regime that are orders of magnitude lower than that of the RCLED.

REFERENCES AND NOTES

1. C. Fabry and A. Perot, *Ann. Chim. Phys.* **16**, 115 (1899).
2. Y. Yamamoto and R. E. Slusher, *Phys. Today* **46** (no. 6), 66 (1993).
3. H. Yokoyama, *Science* **256**, 66 (1992).
4. E. M. Purcell, *Phys. Rev.* **69**, 681 (1946).
5. R. E. Slusher *et al.*, *Appl. Phys. Lett.* **63**, 1310 (1993).
6. S. John, *Phys. Today* **44** (no. 5), 32 (1991).
7. E. F. Schubert *et al.*, *Appl. Phys. Lett.* **61**, 1381 (1992).
8. H. Yokoyama *et al.*, *ibid.* **57**, 2814 (1990).
9. E. F. Schubert, X. H. Wang, A. Y. Cho, L.-W. Tu, G. J. Zydzik, *ibid.* **60**, 921 (1992).
10. F. De Martini, G. Innocenti, G. R. Jacobovitz, P. Mataloni, *Phys. Rev. Lett.* **59**, 2955 (1987).
11. M. Suzuki, H. Yokoyama, S. D. Brorson, E. P. Ippen, *Appl. Phys. Lett.* **58**, 998 (1991).
12. The Golden Rule is a fundamental result of time-dependent perturbation theory for harmonic perturbations. The rule allows one to calculate transition rates in quantum mechanical systems. See, for example, E. Merzbacher, *Quantum Mechanics* (Wiley, New York, ed. 2, 1970).
13. N. E. J. Hunt *et al.*, *Appl. Phys. Lett.* **63**, 2600 (1993).
14. X. P. Feng, *Opt. Commun.* **83**, 162 (1991).
15. See, for example, E. F. Schubert, *Doping in III-V Semiconductors* (Cambridge Univ. Press, Cambridge, 1993).
16. For review, see R. H. Saul, T. P. Lee, C. A. Burrus, in *Semiconductors and Semimetals*, R. K. Willardson and A. C. Beer, Eds. (Academic Press, Orlando, FL, 1985), vol. 22, part C, p. 193.
17. Hewlett-Packard, *Optoelectronics Components Catalogue* (Palo Alto, CA, 1994).
18. T. Kato *et al.*, *J. Cryst. Growth* **107**, 832 (1991).
19. I. Schnitzer, E. Yablonovitch, C. Caneau, T. J. Gmitter, A. Scherer, *Appl. Phys. Lett.* **63**, 2174 (1993).
20. Optical Data Link 50, or ODL 50, is an AT&T product (AT&T part number 1261 AAC).
21. N. E. J. Hunt, E. F. Schubert, D. L. Sivco, A. Y. Cho, G. J. Zydik, *Electron. Lett.* **28**, 2169 (1992).
22. G. Björk, S. Machida, Y. Yamamoto, K. Igeta, *Phys. Rev. A* **44**, 669 (1991).
23. Because the Einstein coefficients $B_{21} = B_{12}$, the gain in a population-inverted structure cannot exceed the loss in a noninverted structure.
24. M. Fukuda, *Reliability and Degradation of Semiconductor Lasers and LEDs* (Artech, Boston, 1991).
25. J. L. Jewell, J. P. Harbison, A. Scherer, Y. H. Lee, L. T. Florez, *IEEE J. Quantum Electron.* **27**, 1332 (1991).
26. T. Kobayashi, T. Segawa, A. Morimoto, T. Sueta, paper presented at the 43rd fall meeting of the Japanese Society of Applied Physics, Tokyo, September 1982.
27. S. L. McCall, A. F. J. Levi, R. E. Slusher, S. J. Pearton, R. A. Logan, *Appl. Phys. Lett.* **60**, 289 (1992).
28. E. Yablonovitch, personal communication.

5 April 1994; accepted 17 June 1994